

# Surprisingly Long-Range Surface-Enhanced Raman Scattering (SERS) on Au–Ni Multisegmented Nanowires\*\*

Wei Wei, Shuzhou Li, Jill E. Millstone, Matthew J. Banholzer, Xiaodong Chen, Xiaoyang Xu, George C. Schatz,\* and Chad A. Mirkin\*

An appropriate wavelength of light impinging on a noble metal nanostructure can cause the conduction-band electrons to oscillate collectively, resulting in localized surface plasmon resonance (LSPR) excitation.<sup>[1,2]</sup> This process generates enhanced electromagnetic (EM) fields at the surface of the nanostructure that can be several orders of magnitude larger than the incident optical excitation fields,<sup>[2–6]</sup> leading to many types of surface-enhanced phenomena,<sup>[3,5,7–14]</sup> including surface-enhanced Raman scattering (SERS). SERS has been extensively studied for several decades,<sup>[5,15]</sup> and it is often described as a near-field phenomenon that occurs when the Raman-active molecules are in proximity to the surface of the nanostructure, as the enhanced EM fields decay rapidly with distance from its surface.<sup>[15–17]</sup> The decay lengths have been reported to be in the range of a few nanometers and depend on the size, shape, and composition of the nanostructure.<sup>[18,19]</sup>

Recently, we developed a process termed on-wire lithography (OWL)<sup>[20]</sup> for the construction of nanostructures from one-dimensional wires by using a template synthesis method.<sup>[21–24]</sup> OWL allows rod and disk structures to be made with sub-5 nm to many micrometers feature size. Importantly, it allows generation of nanostructures over different compositions adjacent to one another. Therefore, OWL allows important distance-dependent phenomena in many areas to be probed,<sup>[25,26]</sup> including molecular electronics, catalysis, spectroscopy, and optics. Indeed, it is an excellent test bed for probing some of the fundamental underpinnings of the SERS phenomenon.

Herein, we describe how OWL can be used to fabricate nanostructures made of gold that have excitable plasmon resonances in the visible region of the spectrum (632.8 nm), and which are separated by nanometer-scale distances from nickel segments that do not have such plasmon resonances but can be selectively modified with Raman-active probes. We have discovered that disklike gold nanostructures can be

separated from the nickel segments by 120 nm and can still exhibit enhanced Raman scattering using the Raman probes, although the probes are only localized on the nickel segment. This is an unprecedented example of long-range SERS. This long-range surface enhancement constitutes a method for using plasmon excitation to enhance photoprocesses over distances that are relevant to applications in chemical and biological sensing.

In a typical experiment, OWL is used to fabricate a 360 nm diameter multisegmented nanowire containing: 1) a 1.5  $\mu\text{m}$  segment of gold, 2) a 1.5  $\mu\text{m}$  gap, 3) a pair of (120  $\pm$  18) nm long gold nanodisks that are separated by a (30  $\pm$  10) nm gap (termed a gold nanodisk pair), and 4) a 1.5  $\mu\text{m}$  nickel wire segment that is separated by a (120  $\pm$  13) nm gap from the gold nanodisk pair (Figure 1a, left to right). The 120 nm gold disk thickness and 30 nm gap distance were chosen based upon previous results from our group that show a near-ideal geometry for obtaining optimized EM enhancement in the context of pure gold structures (that is, in the absence of nickel).<sup>[27]</sup>

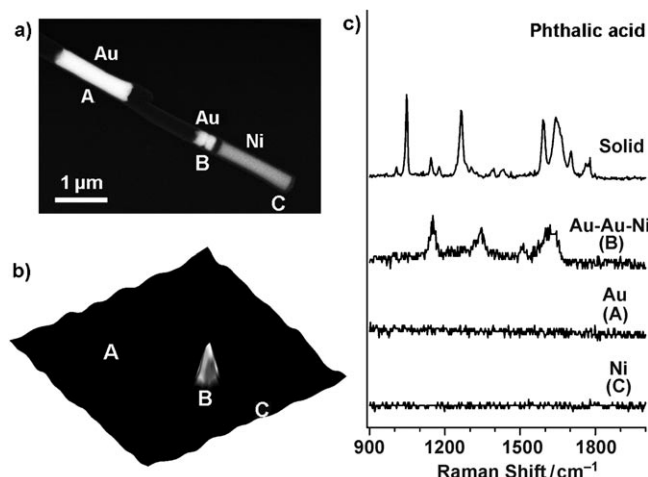


**Figure 1.** a) Scanning electron microscopy image of Au–Ni multisegmented nanowires. Left to right: a 1.5  $\mu\text{m}$  Au nanowire (A); a pair of (120  $\pm$  18) nm long Au nanodisks (B; 360 nm diameter) with a (30  $\pm$  10) nm gap separated by 120  $\pm$  13 nm from a 1.5  $\mu\text{m}$  Ni nanowire (C). The above structures (A and B–C) are separated by a 1.5  $\mu\text{m}$  gap. b) The corresponding confocal Raman microscopy images for nanowires in (a) functionalized with phthalic acid. c) From top to bottom: Raman scattering of phthalic acid in the solid state; SERS of phthalic acid taken from the Ni segment 120 nm from the Au nanodisk pair (point B in (b)); SERS of phthalic acid taken from the individual Au nanowire (point A in (b)) and Ni segment end not associated with the Au nanodisk pair (point C in (b)).

[\*] Dr. W. Wei, Dr. S. Li, J. E. Millstone, M. J. Banholzer, Dr. X. Chen, X. Xu, Prof. G. C. Schatz, Prof. C. A. Mirkin  
Department of Chemistry and International Institute for Nanotechnology, Northwestern University  
2145 Sheridan Road, Evanston, IL 60208-3113 (USA)  
Fax: (+1) 847-567-5123  
E-mail: schatz@chem.northwestern.edu  
chadnano@northwestern.edu

[\*\*] C.A.M. acknowledges the Office of Naval Research (ONR) and the NSSEF program of the DoD for generous financial support. C.A.M. is also grateful for a NIH Director's Pioneer Award. S.L. and G.C.S. were supported by AFOSR/DARPA grant FA9550-08-1-0221.

Supporting information for this article is available on the WWW under <http://dx.doi.org/10.1002/anie.200806116>.

The 120 nm gap between the gold nanodisk pair and the nickel nanowire is noteworthy for several reasons. First, this distance eliminates the possibility of hybridization of the nickel and gold plasmon resonances and the possibility of having accidental overlap with the excitation wavelength. Second, the largest distance for SERS enhancement reported to date is less than 20 nm,<sup>[18,19]</sup> so SERS observations at this distance are new. Third, this distance also allows one to spatially address and determine which segment is responsible for the Raman scattering measured by confocal Raman spectroscopy.

Prior to Raman characterization, these nanostructures were treated with a 20 mM ethanolic solution of phthalic acid (benzene-1,2-dicarboxylic acid) for 24 h (Supporting Information). The carboxylic acid moiety has a strong affinity for nickel but relatively little affinity for gold.<sup>[28–30]</sup> Indeed, confocal Raman imaging of the nanostructures shows a response only from the nickel end adjacent to the gold disk pair (point B, Figure 1b; Figure 1c). Note that no SERS is observed from the gold nanowire (point A, Figure 1b; Figure 1c) or from the individual gold nanodisk pair (Supporting Information, Figure S2). This observation is consistent with the conclusion that the phthalic acid molecules adsorb on the nickel but not on the gold portions of the nanostructure. This also suggests that the SERS enhancement is solely from the nickel nanowire end that is 120 nm from the gold nanodisk pair.

Interestingly, nickel has no SPR modes in the visible region of the spectrum,<sup>[31]</sup> which is consistent with the observation of no  $\lambda_{\max}$  in the dark-field extinction spectrum of a single nickel nanowire (Figure 2) and no SERS from the nickel end that is not adjacent to the gold nanodisk pair (point C, Figure 1b; Figure 1c). Note that the gold nanodisk pair shows broad and intense SPR modes (Figure 2) that are in resonance with the 632.8 nm laser (Figure 2, dotted line).

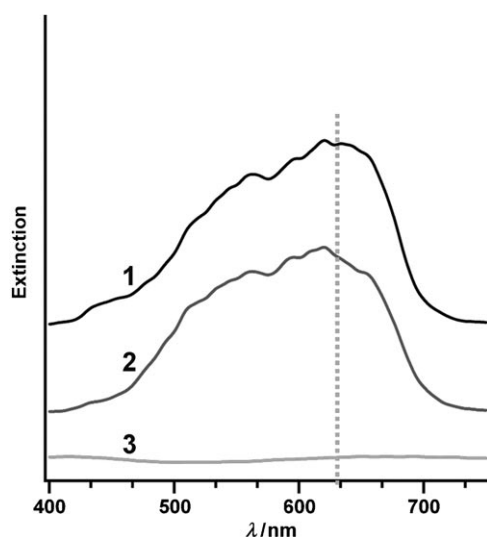


**Figure 2.** Dark-field extinction spectra of an individual Au nanodisk pair (1), a Ni nanowire (3), and a multisegmented nanowire containing an Au nanodisk pair and a Ni nanowire (2). The dotted line indicates the wavelength of the laser (632.8 nm) used to take the Raman spectra.

When the gold nanodisk pair is brought into proximity with the nickel nanowire (separated by 120 nm), the plasmon resonance does not significantly change. This effect is consistent with the conclusion that there is no significant plasmon hybridization between the gold and nickel nanostructures that are separated by 120 nm (Figure 2, curve 2). Since the nickel nanowire alone can not supply SPR-enhanced EM fields to excite the adsorbed phthalic acid molecules, SPR excitation from the nearby gold nanodisk is likely responsible for the observed SERS enhancement.

The above observations are confirmed with another gold–nickel multisegmented nanostructure that contains a 1.5  $\mu\text{m}$  gold nanowire separated by  $(78 \pm 8)$  nm from a 2.0  $\mu\text{m}$  nickel nanowire (Supporting Information, Figure S3). The weaker SERS intensity (compared to the gold nanodisk pair–nickel, Figure 1) is possibly due to poorer overlap between  $\lambda_{\max}$  of the gold nanowire and the incident wavelength (632.8 nm, red dotted line, Supporting Information, Figure S3(c)).

Theoretical modeling studies strengthen our conclusions. The effect of the gold nanodisk pair on the SERS intensity associated with the nearby nickel nanowire can be inferred by comparing the  $|E|^4$  enhancement on the nickel surface (Supporting Information, Figure S4; nickel nanowire 120 nm from a gold nanodisk pair) with the corresponding enhancement for a nickel nanowire in the absence of the gold nanodisk pair. Our calculations show that the  $|E|^4$  enhancement factor (averaged over the surface) is 30 for the gold nanodisk pair–nickel structure (Supporting Information, Figure S3), whereas it is only 10 for the nickel nanowire in the absence of the gold nanodisk pair. This enhancement demonstrates that the gold nanodisk pair produces significant enhancement in the SERS intensity (factor of ca. 3) associated with the nearby surface of the nickel nanowire. Thus, the direct transfer of excitation from the gold nanodisk pair to the nickel nanowire is what leads to the SERS enhancement in the experimental observation.

The observed long-range enhancement leads to a more comprehensive understanding of the SPR-enhanced EM fields with the distance from the surface of the nanostructure. SERS has been often thought of as having a range of a few nanometers from the nanostructures, as the previous studies were conducted by applying spacing materials between the Raman molecules and the surface of the nanomaterials.<sup>[19,32]</sup> These spacing materials with higher dielectric constants (relative to air) lead to rapid decay of EM fields away from the nanostructures,<sup>[15]</sup> making it difficult to interrogate the relationship between the enhanced EM fields and the distance from the surface. In our approach, the probe molecules were separated from the SPR nanomaterials without high-index spacing materials, which allows for the realization of much longer SERS distances (120 nm from the gold nanodisk pair).

These observations are fundamentally interesting and potentially technologically important. Traditionally, SPR-enhanced detection has been limited to the relatively few materials that have visible plasmon resonances and provide very large field enhancement (e.g. gold and silver). Using this long-range SERS, one can now consider strategies for probing reactions on SERS-inactive materials with adjacent noble

metal nanostructures that are separated by distances that minimize quenching (in the case of fluorophores) but still allow for significant SPR field enhancement.

## Experimental Section

Multisegmented nanostructures were prepared by using the OWL method.<sup>[20]</sup> In a typical experiment, 360 nm diameter Au-Ag-Au-Ag-Ni nanowires were synthesized by template-directed electrochemical synthesis,<sup>[21–24]</sup> and then half-coated with a 50 nm thick silica (SiO<sub>2</sub>) layer by plasma-enhanced chemical vapor deposition (PECVD). After silica deposition, the sacrificial Ag segments were dissolved, which created gaps between the Au–Au and Au–Ni segments along the long axes of the nanowires. The Ag etching and silica coating were confirmed by SEM/EDX (scanning electron microscopy/energy dispersive X-ray spectroscopy). In the OWL process, the length of each segment can be precisely controlled simply by controlling the charge (number of Coulombs) passed during electrochemical deposition. Segment number and composition also can be controlled so that it is easy to prepare wires with multiple gaps, gaps of different lengths,<sup>[33]</sup> and segments of different compositions.

Phthalic acid (benzene-1,2-dicarboxylic acid) was selected as the Raman-active molecule because the carboxyl group adsorbs onto Ni but not Au surfaces.<sup>[28,34]</sup> To effectively modify the surface with phthalic acid, the nanowires were first isolated from an ethanol solution by centrifugation, and then resuspended in a 100  $\mu$ L ethanol solution of phthalic acid (20 mM) and shaken for 24 h. The phthalic acid modified nanowires were subsequently isolated by centrifugation and repeatedly washed with ethanol to remove free and physisorbed phthalic acid, and then cast onto piranha-pretreated glass substrates.

Raman spectra and images were recorded with a confocal Raman microscope (Alpha, WiTec Instruments) equipped with a piezo scanner and 100 $\times$  microscope objective (NA = 0.90, Nikon, Tokyo, Japan).<sup>[27]</sup> The spatial resolution was 300 nm in this experiment. Samples were excited using a He-Ne laser (632.8 nm, Coherent Inc., Santa Clara, CA) with a spot size of about 1  $\mu$ m and a power density of about 10<sup>4</sup> W cm<sup>-2</sup> on the samples. For a typical Raman image with a scan range of 15  $\mu$ m  $\times$  15  $\mu$ m, complete Raman spectra were acquired on every pixel with an integration time of 0.3 s per spectrum and an image resolution of 100 pixels  $\times$  100 lines. To provide a careful analysis of the enhanced Raman scattering signal of phthalic acid on the sample features, all images presented here were processed by integrating the intensity of the Raman spectra at 1346 cm<sup>-1</sup> (Supporting Information, Figure S1), which is attributed to the  $\nu_s(\text{COO}^-)$  mode of the carboxylate group.<sup>[35]</sup> The microscopic length of the nanowire allows one to spectroscopically address and distinguish each set of nanostructures decorating the silica layer backing along the long wire axis independently. The experiments have been reproduced multiple times, with additional measurements on more OWL-fabricated multisegmented nanowires.

The dark-field extinction spectra of a single Au nanowire, a single Au nanodisk pair, a single Ni nanowire, and a Au–Ni multisegment nanowire were acquired using a Zeiss microscope (Axiovert 100 A) equipped with a CRAIC spectrometer (QDI301) and 100 $\times$  microscope objective (NA = 0.90, Nikon, Tokyo, Japan). A halogen lamp (HAL 100) was used as the light source.

Received: December 15, 2008

Published online: May 8, 2009

**Keywords:** nanowires · on-wire lithography · surface chemistry · surface plasmon resonance · surface-enhanced Raman scattering

- [1] U. Kreibitz, M. Vollmer, *Optical Properties of Metal Clusters*, Springer, Berlin, **1995**.
- [2] H. Raether, *Surface Plasmons*, Springer, New York, **1988**.
- [3] J. Aizpurua, W. B. Garnett, J. R. Lee, F. J. G. d. Abajo, K. K. Brian, T. Mallouk, *Phys. Rev. B* **2005**, *71*, 235420.
- [4] J. R. Krenn, *Nat. Mater.* **2003**, *2*, 210.
- [5] M. Moskovits, *Rev. Mod. Phys.* **1985**, *57*, 783.
- [6] P. I. Geshev, U. C. Fischer, H. Fuchs, *Opt. Express* **2007**, *15*, 13796.
- [7] C. J. Murphy, A. M. Gole, S. E. Hunyadi, J. W. Stone, P. N. Sisco, A. Alkilany, B. E. Kinard, P. Hankins, *Chem. Commun.* **2008**, 544.
- [8] S. Eustis, M. El-Sayed, *J. Phys. Chem. B* **2005**, *109*, 16350.
- [9] P. Alivisatos, *Nat. Biotechnol.* **2004**, *22*, 47.
- [10] J. Jiang, K. Bosnick, M. Maillard, L. Brus, *J. Phys. Chem. B* **2003**, *107*, 9964.
- [11] Y. C. Cao, R. Jin, C. A. Mirkin, *Science* **2002**, *297*, 1536.
- [12] C. D. Keating, K. M. Kovaleski, M. J. Natan, *J. Phys. Chem. B* **1998**, *102*, 9404.
- [13] S. M. Nie, S. R. Emory, *Science* **1997**, *275*, 1102.
- [14] D. Graham, K. Faulds, *Chem. Soc. Rev.* **2008**, *37*, 1042.
- [15] K. A. Willets, R. P. Van Duyne, *Annu. Rev. Phys. Chem.* **2007**, *58*, 267.
- [16] Y. Fang, Y. Wei, C. Bai, L.-s. Kan, *J. Phys. Chem.* **1996**, *100*, 17410.
- [17] Z.-Q. Tian, B. Ren, J.-F. Li, Z.-L. Yang, *Chem. Commun.* **2007**, 3514.
- [18] G. Barbillon, J. L. Bijeon, J. S. Bouillard, J. Plain, M. Lamy De La Chapelle, P. M. Adam, P. Royer, *J. Microsc.* **2008**, *229*, 270.
- [19] J. A. Dieringer, A. D. McFarland, N. C. Shah, D. A. Stuart, A. V. Whitney, C. R. Yonzon, M. A. Young, X. Zhang, R. P. Van Duyne, *Faraday Discuss.* **2006**, *132*, 9.
- [20] L. Qin, S. Park, L. Huang, C. A. Mirkin, *Science* **2005**, *309*, 113.
- [21] G. E. Possin, *Rev. Sci. Instrum.* **1970**, *41*, 772.
- [22] C. K. Preston, M. Moskovits, *J. Phys. Chem.* **1993**, *97*, 8495.
- [23] S. J. Hurst, E. K. Payne, L. Qin, C. A. Mirkin, *Angew. Chem.* **2006**, *118*, 2738; *Angew. Chem. Int. Ed.* **2006**, *45*, 2672.
- [24] C. R. Martin, *Science* **1994**, *266*, 1961.
- [25] X. Chen, Y.-M. Jeon, J.-W. Jang, L. Qin, F. Huo, W. Wei, C. A. Mirkin, *J. Am. Chem. Soc.* **2008**, *130*, 8166.
- [26] W. Wei, S. Li, L. Qin, C. Xue, J. E. Millstone, X. Xu, G. C. Schatz, C. A. Mirkin, *Nano Lett.* **2008**, *8*, 3446.
- [27] L. Qin, S. Zou, C. Xue, A. Atkinson, G. C. Schatz, C. A. Mirkin, *Proc. Natl. Acad. Sci. USA* **2006**, *103*, 13300.
- [28] Y. Sakata, K. Domen, K. Maruya, T. Onishi, *Catal. Lett.* **1990**, *4*, 169.
- [29] L. A. Bauer, D. H. Reich, G. J. Meyer, *Langmuir* **2003**, *19*, 7043.
- [30] A. K. Salem, P. C. Searson, K. W. Leong, *Nat. Mater.* **2003**, *2*, 668.
- [31] B. Ren, G.-K. Liu, X.-B. Lian, Z.-L. Yang, Z.-Q. Tian, *Anal. Bioanal. Chem.* **2007**, *388*, 29.
- [32] A. V. Whitney, J. W. Elam, S. Zou, A. V. Zinovev, P. C. Stair, G. C. Schatz, R. P. Van Duyne, *J. Phys. Chem. B* **2005**, *109*, 20522.
- [33] C. R. Martin, L. A. Baker, *Science* **2005**, *309*, 67.
- [34] A. K. Salem, P. C. Searson, K. W. Leong, *Nat. Mater.* **2003**, *2*, 668.
- [35] E. Tourw, K. Baert, A. Hubin, *Vib. Spectrosc.* **2006**, *40*, 25.